EUROfusion

EUROFUSION CP(15)04/08

E. Fortuna-Zaleśna et al.

Dust Survey Following the Final Shutdown of TEXTOR: Metal Particles and Fuel Retention

(18th May 2015 – 22nd May 2015)
Aix-en-Provence, France

This work has been carried out within the framework of the EUROfusion Consortium and has received funding from the Euratom research and training programme 2014-2018 under grant agreement No 633053. The views and opinions expressed herein do not necessarily reflect those of the European Commission.

Dust survey following the final shutdown of TEXTOR: Metal particles and fuel retention

E. Fortuna-Zaleśna[a*], A. Weckmann[b], J. Grzonka[a], M. Rubel[b], H.G. Esser[c], M. Freisinger[c], A. Kreter[c], G. Sergienko[c], P. Ström[b]

[a]*Faculty of Materials Science and Engineering, Warsaw University of Technology, Warsaw, Poland*

[b]*Department of Fusion Plasma Physics, Royal Institute of Technology (KTH), 100 44 Stockholm, Sweden*

[c]*Institut für Energie- und Klimaforschung, IEK-4, Plasma Physics, Forschungszentrum Jülich, 52425 Jülich, Germany*

Abstract

The work presents results of a broad TEXTOR dust survey in terms of its composition, structure, distribution and fuel content. The dust particles were collected after final shutdown of TEXTOR in December 2013. Fuel retention, as determined by thermal desorption, varied significantly, even by two orders of magnitude, dependent on the dust location in the machine. Dust structure was examined by means of scanning electron microscopy combined with energy-dispersive X-ray spectroscopy, focused ion beam and scanning transmission electron microscopy. Several categories of dust have been identified. Carbon-based stratified and granular deposits were dominating, but the emphasis in studies was on metal dust. They were found in the form of small particles, small spheres, flakes and splashes which formed "comet"-like structures clearly indicating directional effects in the impact on surfaces of plasma-facing components. Nickel-rich alloys from the Inconel liner and iron-based ones from various diagnostic holders were the main components of metal-containing dust, but also molybdenum and tungsten debris were detected. Their origin is discussed.

Keywords: *TEXTOR, dust, fuel retention, high-Z metals*

Corresponding author: e.fortuna@inmat.pw.edu.pl

1. Introduction

The main driving force for dust studies in tokamaks has been related to safety issues and – in a consequence – was of paramount importance in licensing process of ITER in connection with a planned operation with a deuterium-tritium fuel. Very detailed dust surveys have been carried out regularly at several tokamaks: TEXTOR [1-8], ASDEX-Upgrade [9-11] and Tore Supra [12] and other machines, as summrised by Braams [13]. The concern regarding fuel invenotry [14,15] followed by decision of ITER to operate from day 1 with plasma-facing components (PFCs) made of beryllium (Be) and tungsten (W) has strongly shifted the interest in dust studies towards metal particles: origin, shape, size distribution, clustering and material mixing, i.e. intermetallic compounds and mixes with low-Z plasma impurities.

The final shut-down of the TEXTOR tokamak (December 2013) has offered nearly unlimited possibilities to perform a very detailed fuel retention studies and dust survey. The tokamak was operated with main PFCs made of carbon, but the machine's scientific mission was strongly oriented towards material testing. It included especially high-Z metals such as tungsten and molybdenum: test limiters made of solid metal [16-26] or coatings on carbon-based substrates [26-28], controlled injection of metal dust [29] or puffing gases containing heavy metals, i.e. hexafluorides of W [30] and Mo [31]. The latter injection experiment preceded the final shut-down during which a large number of wall tiles and probes [32] were removed and dust was sampled from different locations. This paper is focused on two aspects of dust examination: fuel content and comprehensive characterisation of especially metal particles: their composition, structure including internal features of droplets and splashes.

Experimental

2.1 Dust collection

The investigations were carried out on samples retrieved from the TEXTOR tokamak after its final shutdown in December 2013. Dust collection was the first action performed after venting the vacuum vessel and radioactivity measurements before allowing the man entry. It has been well known from earlier studies [1-8] that the major component of dust particles would be carbon. Therefore, no particular effort was associated with the quantification of dust. The interest was in sampling from a large number of locations. Sampling was performed manually

by collecting loose matter from pump ducts underneath the main toroidal belt pump limiter ALT-II (Advanced Limiter Test), by scraping deposits from the wall (e,g. from the liner) and ALT-II blade backsides or by applying adhesive carbon tape, i.e. carbon sticky pads. Samples originate from various positions on the liner and the main limiter tiles: backside of toroidal ALT-II, main poloidal limiters, RF antenna protection limiter of ion cyclotron antenna and from the inner bumper being a shield of the dynamic ergodic divertor (DED). More than 200 samples collected from over 20 locations have been studied. Details regarding the location and the type of study are given in Table 1 for samples described in this paper. Location is given in terms of : (a) the toroidal angle (Θ) in the plasma current direction under normal operation shown with respect to the position of the Limiter Lock (LL1) where test limiters and gas injection experiments were carried out; (b) poloidal angle (ϕ) with respect to the outer equatorial plane, i.e. on the low field side (LFS).

Table 1. A list of samples with results reported in the paper: sample location in terms of poloidal and type of study. Term „Microscopy" denotes a set of techniques including SEM, EDS, FIB and STEM.

Sample	**Torus location**[#)]		**Location**	**Type of study**
	Θ [°]	φ [°]		
1 (1)	-165	+100	Liner, vessel top	Microscopy
2 (13)	-85	+60	Liner, LFS, within a dust specimen	Microscopy
3 (14)	-85	+45	Liner, LFS, within a dust specimen	Microscopy
4 (22)	+45	+15	Liner, LFS	Microscopy
5 (27)	-55	+45	Liner, LFS	Microscopy
6 (28)	+40	+40	Liner, LFS	Microscopy
7 (33)	+165	+10	Liner, vessel bottom	Microscopy
8 (34)	+165	+70	Liner, LFS	Microscopy
9 (B02)	+20	+10	Limiter side, LFS	TDS
10 (B03)	-75	+90	Liner bulge close to DED bridge, vessel top	TDS
11 (B05)	-10	+50	RF antenna limiter side	TDS
12 (B10)	+170	+10	Liner bulge close to RF antenna	TDS
13 (B13)	+10	+85	Liner bulge, vessel top	TDS
12 (5)	-165	+80	Top antenna limiter	Microscopy
13 (9)	-155	+150	On inner bumper limiter tile, HFS	Microscopy
14 (23)	-160	-90	Part of the DED bridge, vessel bottom	Microscopy
15 (36)	-160	+90	DED bridge limiter, vessel top	Microscopy
16 (37)	-65	+90	DED bridge limiter, vessel top	Microscopy
17 (38)	+25	+90	DED bridge limiter, vessel top	Microscopy
18 (39)	**+25**	**-90**	**DED bridge limiter, vessel bottom**	Microscopy
19 (ALT2)	-	-	Scraping from backside of ALT blade 2	Microscopy

20 (ALT4)	-	-	Scraping from neutraliser plates (ALT blade 4)	Microscopy
21 (H1)	-85	-35	Backside of ALT blade 7	Microscopy
22 (H2)	-80	-39	Backside of ALT blade 7	Microscopy
23 (H3)	-78	-42	Backside of ALT blade 7	Microscopy
24 (H5)	**-74**	**-48**	**Backside of ALT blade 7**	Microscopy

[#)] With respect to the limiter lock LL1, θ in plasma current direction under normal configuration, ϕ=0° on the outer equator (90° = up, -90° = down)

2.2. Analysis methods

The study was performed using a broad range of microscopy methods and by thermal desorption spectrometry (TDS). In microscopy studies the main focus was on the presence of metals: especially tungsten and molybdenum, but also nickel associated with Inconel structures in TEXTOR (liner and antenna grill) and steel from holders of various in-vessel diagnostics. 25 samples were chosen (see Table 1) for microscopy studies. Scanning electron microscopy (Hitachi SU-70 FE-SEM) was combined with energy-dispersive X-ray spectroscopy (EDS Thermo Scientific Ultra Dry, type SDD) and YAG BSE (backscattered electrons) detector. The internal morphology of selected particles was determined by means of focused ion beam (FIB/SEM Hitachi NB5000) and scanning transmission electron microscopy (STEM, Aberration Corrected Dedicated STEM Hitachi HD-2700) techniques. Another five specimens were outgassed to determine deuterium content in various locations. TDS was performed using the Prisma (Pfeiffer Vacuum) and MKS mass spectrometers. The outgassing was done in three steps: around 2000 s at 323 K, increase to 423 K and baking for 3000-7000 s and then fast temperature increase to 1273 K.

Results and discussion

3.1. Microstructure of dust and debris

The microstructures of co-deposits collected from the liner (bottom of the machine) and from bottom part of the ALT-II Inconel blade are shown in Fig. 1(a) and (b), respectively. The structure of these two distinct types of carbon-based deposits, stratified and columnar/granular, is related to the temperature in the zone where the layers were formed. Laminar structures occur at surfaces where temperature usually does not exceed 600 K, while the granular are typical for high temperature range (even 2000 K), as discussed in [7,33]. The co-deposits present at samples from the ALT tiles and the vicinity of the limiter are rich in

carbon, boron and oxygen whereas these from the liner, bottom part of the Inconel blades are rich in silicon. The presence of Fe, Ni, Cr is detected by EDS in all types of deposits.

In case of boron-rich 50-150 nm thick layers collected from the liner amorphous structure has been observed, as exemplified in Fig. 2. There is also a very clear 15 nm thick interlayer containing mainly tungsten, appearing as a bright stripe in the image recorded high-angle-annular dark field (HHADF) STEM. While the boron-containing strata originate from the regular boronisation of TEXTOR [34] and their presence has been well documented in the past [35], a distinct W stratum has been detected for the first time. Its formation is most probably associated with one of earlier WF_6 puffing experiments for high-Z transport studies [30] or/and spectroscopy calibration. The layer, on the scale analyzed, is fairly uniform and its presence does not lead to splitting of the deposit into separate thin layers.

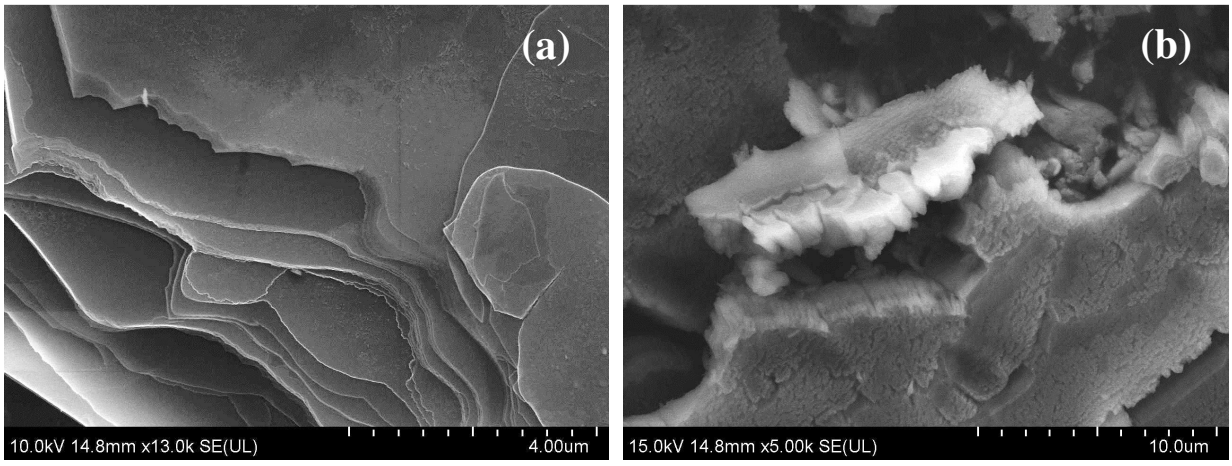

Fig. 1. (a) Stratified deposit from the liner and (b) columnar structure from the bottom part of the ALT-II support blade.

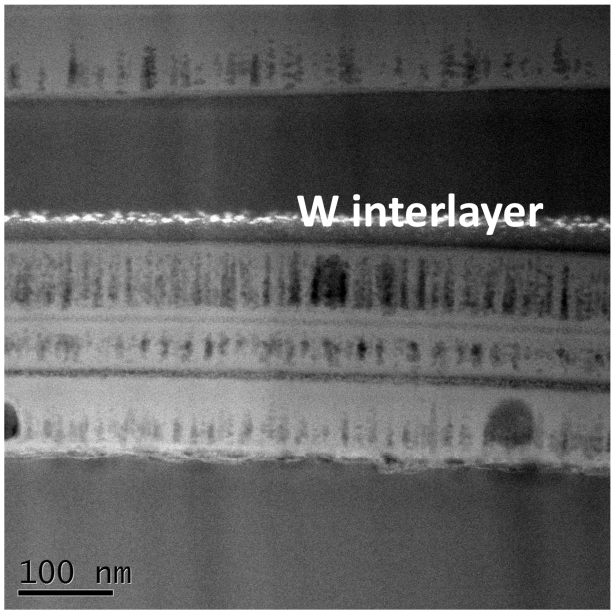

Fig. 2. HAADF STEM image of boron rich co-deposit structure W-rich interlayer in the do-deposit formed on the liner.

Concerning metal dust, iron-based particles appear in the largest number. They are dominant in matter collected from the ALT tiles. In addition to iron they contain chromium and nickel, typical components of stainless steel. This is most probably related to the material damage, melting and splashing, of various steel-made diagnostic holders when they suffer from disruptions and even human errors in the manipulator positioning. The detected particles include small metallic spheres, splashed droplets, irregular particles and flakes (size: 0.2-30 μm), as documented in Fig. 3 (a-d). Especially in Fig. 3 (a) and (b) one can clearly see that metal was molten and droplets were deposited on surfaces. It should be stressed that bigger metal debris and swarf (up to mm size, as reported in [7]) originating from the in-vessel work are not taken into account in the current work. The internal structure of a splashed Fe-based particle is shown in Fig. 4. It is a polycrystalline material with small, equiaxial grains, 60-200 nm in diameter. At particle surface ca. 30 nm thick amorphous zone is present.

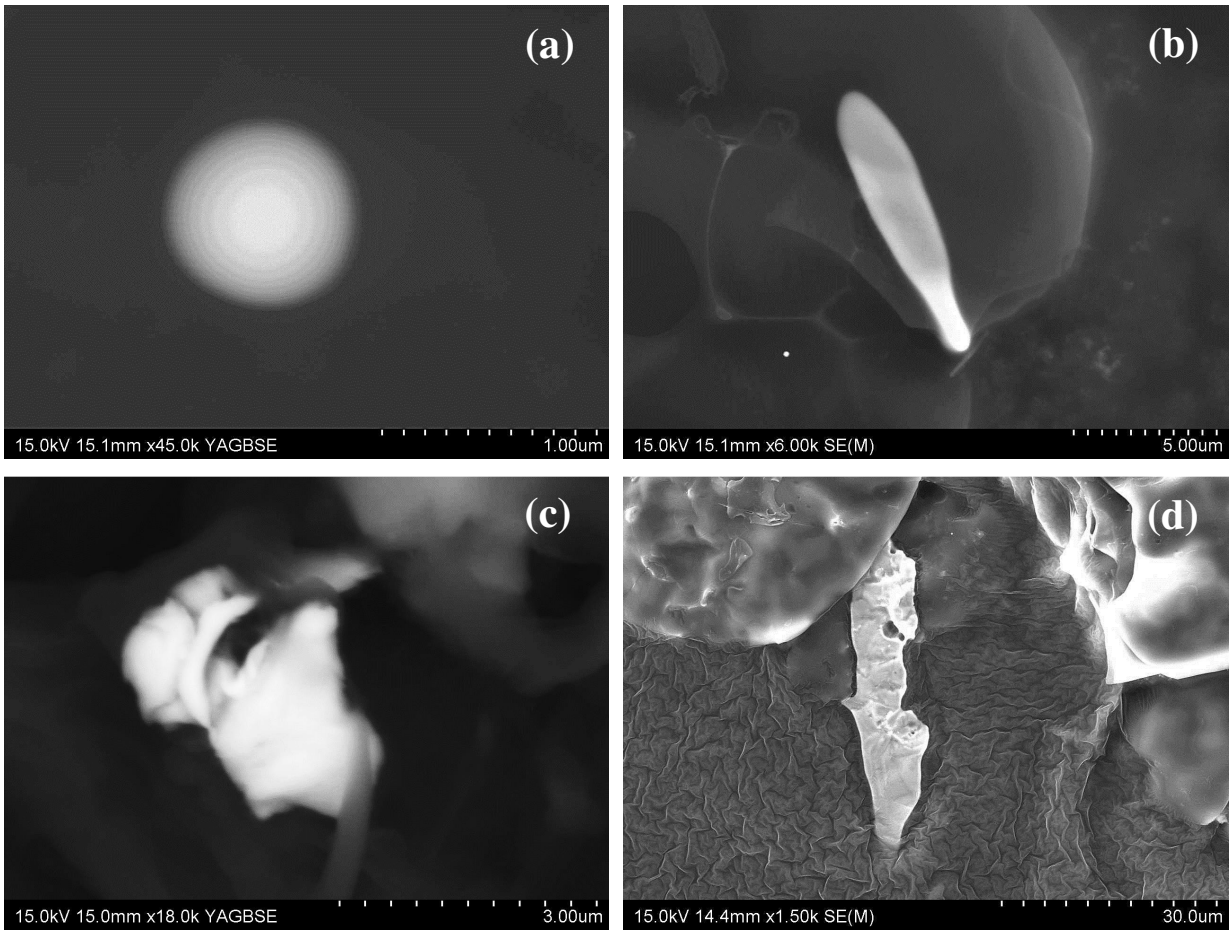

Fig. 3. Microstructure of Fe-based particles.

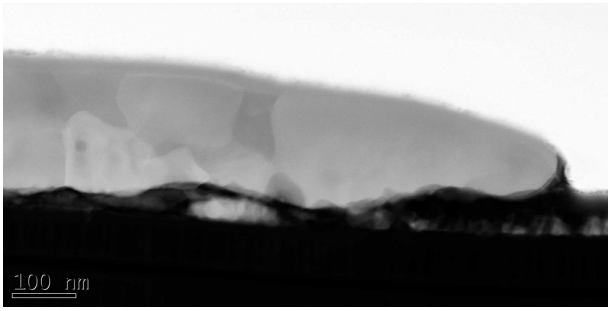

Fig. 4. STEM image of a splashed Fe-based particle (Z-contrast mode) in the sample collected from the liner.

The second largest group are nickel based particles detected in deposits originated from the liner and bottom part of the Inconel blades. These particles are predominantly in the form of irregular flakes and small spheres (SEM images in Fig. 5) just clearly proving that the metal debris was transported in plasma. Their size varies from 0.3 to 7 μm. The composition of majority of these particles corresponds to nickel alloy Inconel 625 thus suggesting that they are erosion products from the liner or ICRF antenna grill. A large fraction of these particles

contain also molybdenum (3-10.5 wt. %). The structure of an irregular nickel-based particle is presented in Fig.6. It is polycrystalline with small equiaxial grains, 75-200 nm in diameter.

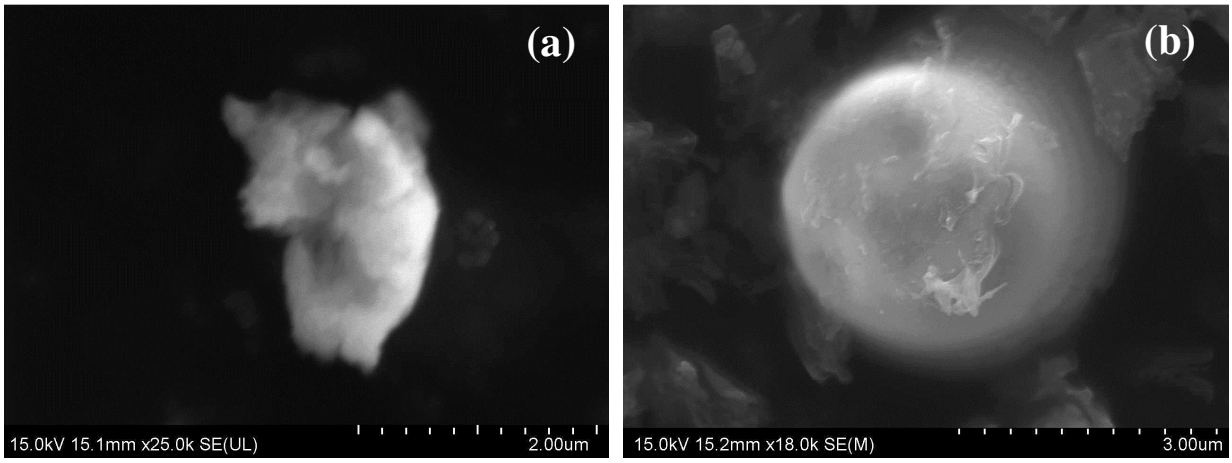

Fig. 5. SEM images of Ni-based particles

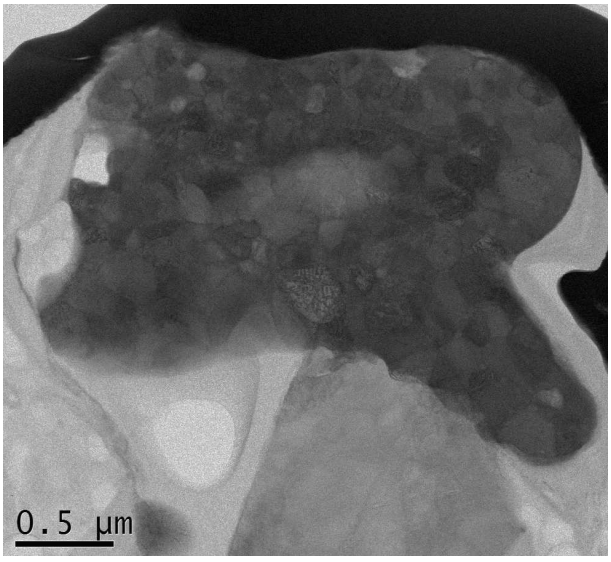

Fig. 6. Bright field STEM image of the internal structure of an Inconel particle collected from the back side of the ALT-II supporting blade.

A particular interest was on the identification of objects consisting molybdenum and tungsten. The presence of Mo-based particles has been identified in all examined samples (see Table 1). Their mean size of such particles is about 4.5 µm and they are characterised by a layered structure, as shown in Fig.7a. The internal structure of these particles was investigated via observations of two lamellae prepared by FIB. Bright field STEM image of the particle structure is presented in Fig. 7b. In the material sublayers, 80-150 nm thick, are clearly detected. Molybdenum was also found in sub-micron spherical particles as shown in Fig. 8.

The most probable origin of the molybdenum debris is the erosion of meshes in the neutral beam injection system.

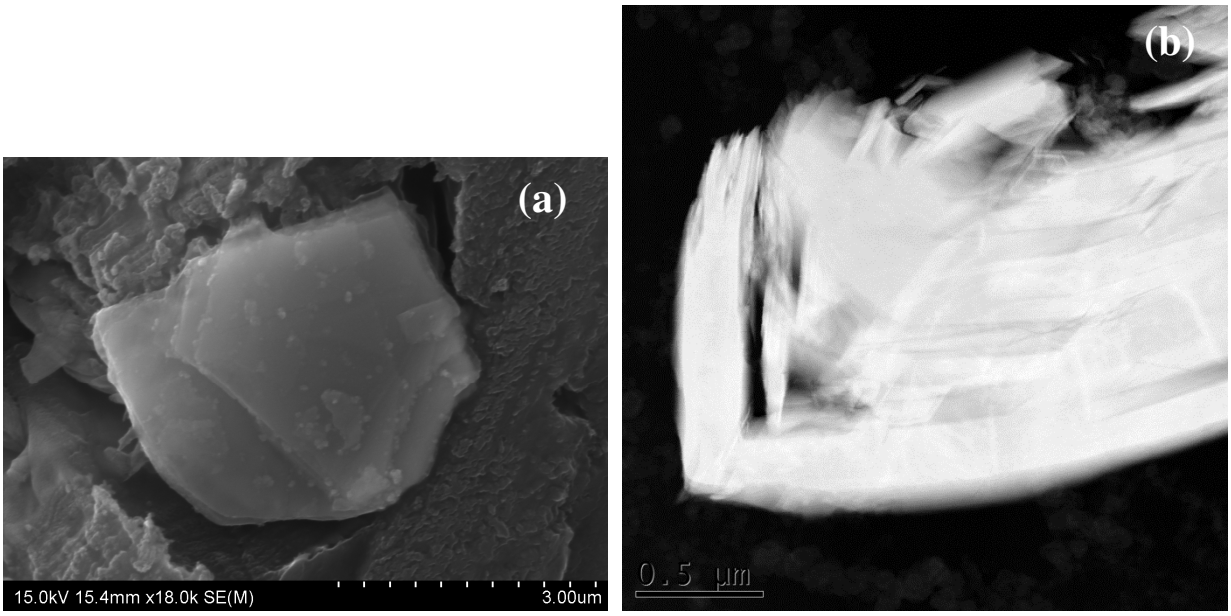

Fig. 7. Mo-based particle of a layered structure: (a) topography; (b) HAADF STEM image.

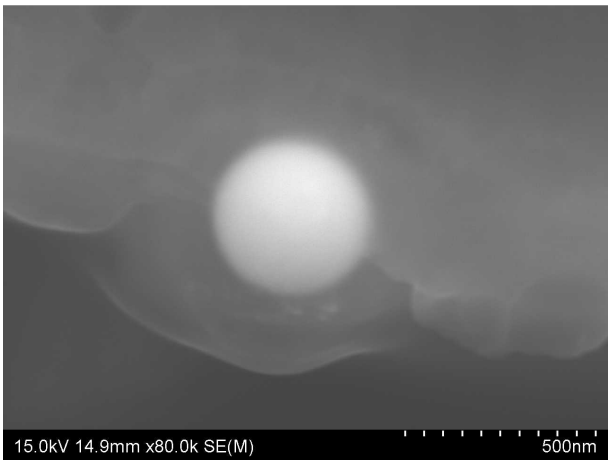

Fig. 8. Small regular Mo sphere.

Tungsten based particles were hardly detected at the surface. Single particles were found only in a few samples. The reason of difficulties in tungsten based particles detection could be their small size, as described in the following. The observed morphology included: spherical particles, irregular, particles with tungsten layer, fine particles in carbon matrix, Fig. 9 (a-d). These were small particles of the size in the range 0.3-1.2 µm. The only location where more W of particles could be found was the bottom DED shield located near the manipulator (Limiter Lock LL1 [36]) used for material testing and variety of other experiments including gas or dust injection [29-32]. In that case larger particles of several microns were detected

(size 1.5-7 μm). In general, the origin of W particles is associated with exposures of tungsten test limiters [20-25, 37] of many types, when also melting occurred especially in experiments designated to testing material limits under plasma exposure. Another history is may be associated with the W object in Fig. 9(d). It is size and shape and irregular shape suggests that it is tungsten grain used in the controlled dust injection experiment [29]. One may infer that the particle probably did not enter plasma and its surface was not ablated.

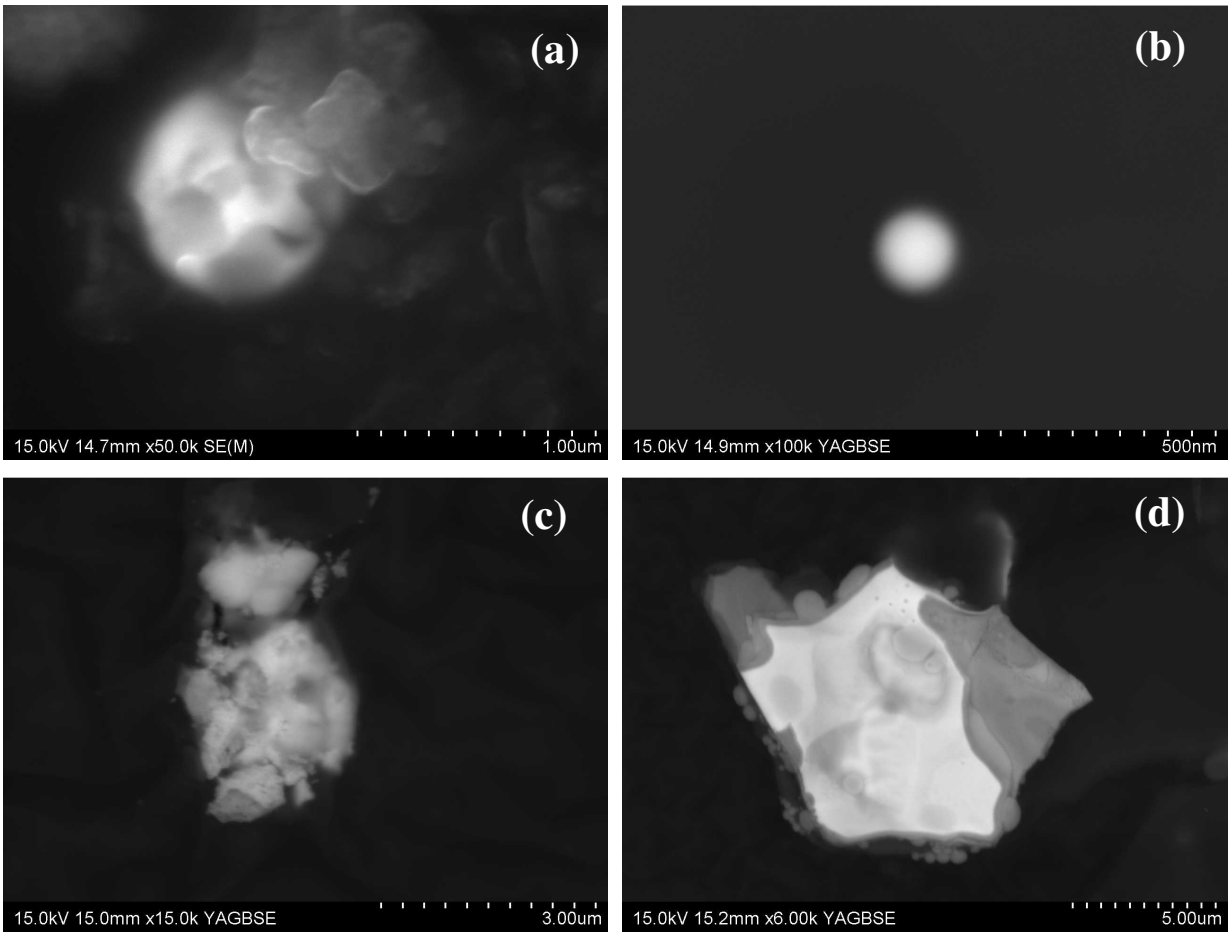

Fig. 9. Microstructure of various W-based particles.

3.2. Metal splashes

Micrographs in Fig. 10 and 11 show two categories of metal splashes on the limiters and on the liner: irregular objects of the size of up to 100 μm and elongated "comet-like" structures, respectively. Arrows in Fig 10 mark the direction of the plasma flux the surface as can be deduced from orientation of the columnar structures of carbon-rich deposits on the metal splashes. It indicates that splashes resided on the ALT-II surfaces for some time and were covered by deposits. In the case of the "comets" one may conclude that they are most probably created by small metal droplets which move with high speeds and collide under low

grazing angle with the surface. Another explanation could be that these structures appeared due to the JxB forces associated with secondary electron current which is acting on molten metal droplets attached to the surface [23]. Such thermo-electron currents play essential role only above 3000K which is the boiling point of iron. In examples shown in Fig.10(a) and Fig.11(b), JxB force could be associated with thermo-electron currents because this metal splash has a number of small bubbles thus clearly indicating the boiling process. In Fig.11(a) there are many small splashes having different orientations, but all are moved up. Therefore, they could be created during plasma disruption when magnetic field direction can change quickly if plasma moves towards this surface. It could be also combination of the two cases discussed above: the droplet collides with surface under a small angle and then starts moving due to the combined action of JxB and inertia forces. The latter case is the most probable taking into account small angular spread of the "comet-like" structures which is below 60°.

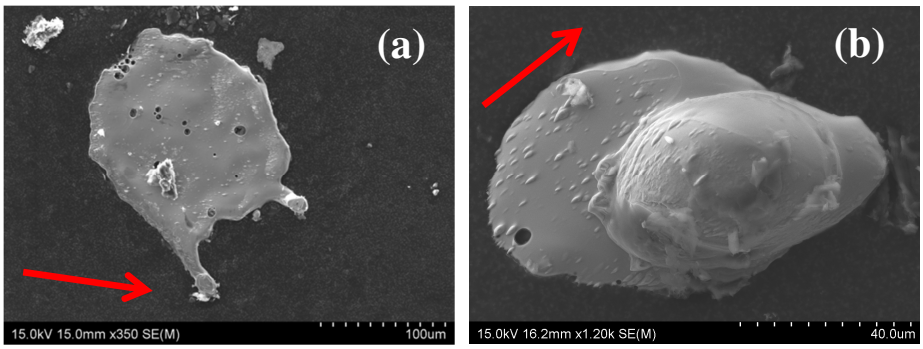

Fig. 10. Splashes of steel on ALT limiter surface. Red rows show the direction of the plasma flux.

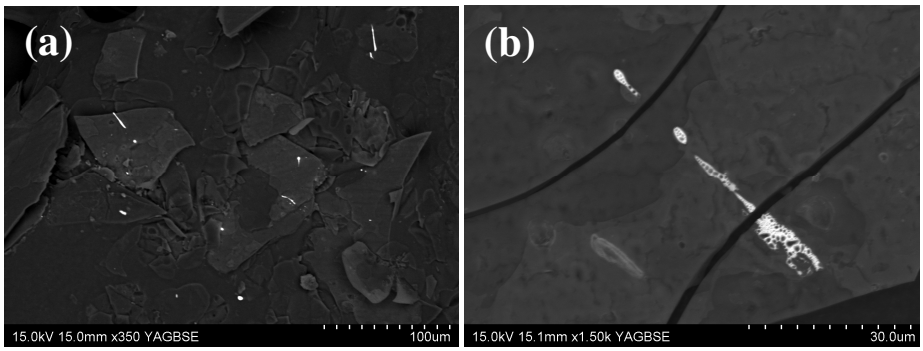

Fig. 11. Examples of "comet-like" splashes of stainless steel identified in many samples.

3.3. Fuel content

Thermal desorption was performed for five samples of deposits removed by scraping from the Inconel liner and the graphite tiles protecting DED installation on top of the vessel and the RF antenna. Two specimens from each dust sample were outgassed. The amount of material taken

for outgassing in each run was in the milligram range: 1.3 – 5.8 mg. Data in Table 2 inform about the amount deuterium in atoms per gram of carbon deposit and the respective concentration ratio D/C. Plots in Fig. 12 (a) and (b) show the desorption characteristics.

Table 2. Retention of deuterium in co-deposits from various locations. The atomic density of carbon is 4.5 10^{22} g^{-1}.

Sample Location	Amount outgassed (g)	D content (10^{20} at/g C)	D/C ratio#
9 (B02) side of top DED limiter	0.00173323 0.00286178	0.7 3.4	0.001 0.007
10 (B03) liner close to limiter	0.00206808 0.00560546	1.3 5.2	0.003 0.001
11 (B05) RF antenna	0.00446896 0.00570570	0 0	0 0
12 (B10) liner close to RF	0.00170120 0.00182516	8.3 11.2	0.017 0.022
13 (B13) liner close to limiter	0.00138073 0.00490954	0.8 0.3	0.002 0.001

#) *assuming carbon as the main dust component.*

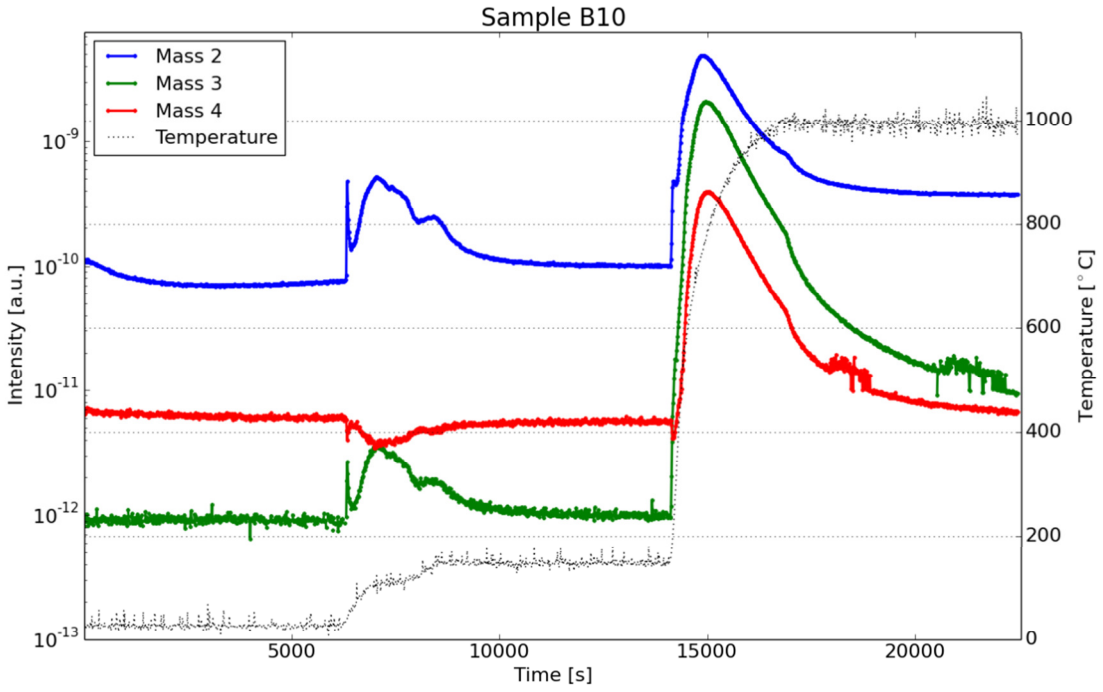

a)

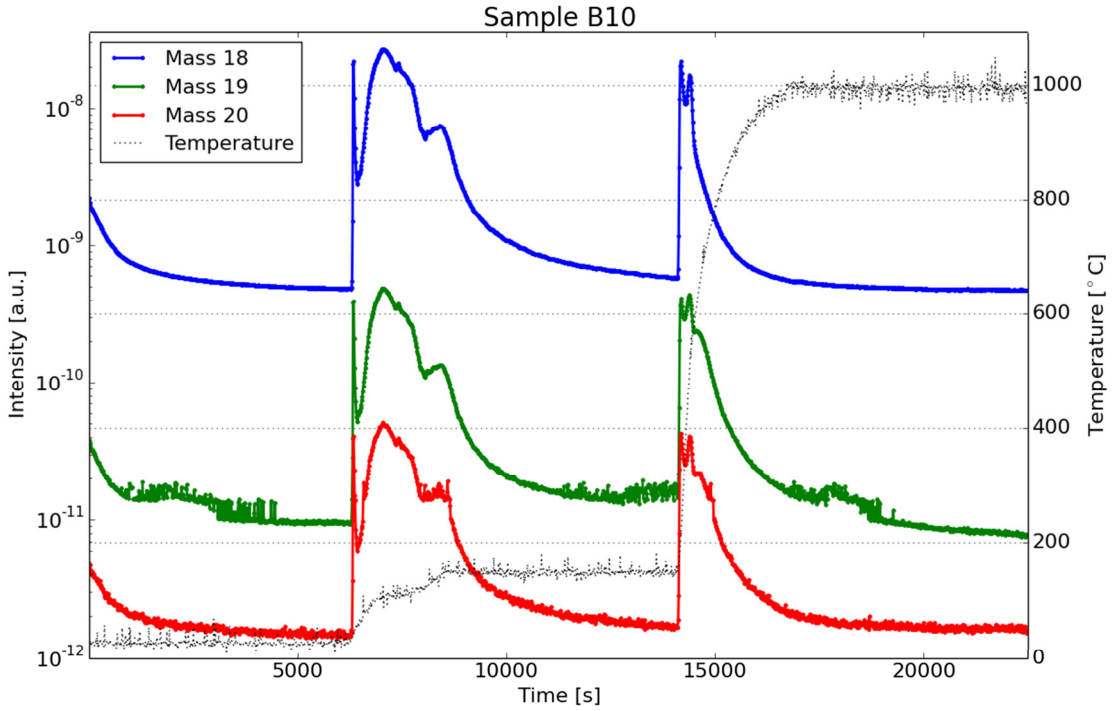

b)

Fig. 12. Desorption characteristics from sample 12 (B10) for: (a) hydrogen species M2, M3 and M4 and (b) water group M18, M19 and M20 with two hydrogen isotopes. No background subtraction has been applied.

There are a few important messages related to TDS. For specimens taken from the same sample D content may vary even by a factor of 5 thus indicating that probably small differences in the structure have a strong impact on the fuel retention. There are big differences between samples collected from the liner, from 0.3×10^{20} at/g to 11.2×10^{20} at/g. As could be expected, no deuterium is detected on the sample taken from the RF antenna protection limiter which was at high temperature during plasma operation.

The deuterium-to-carbon concentration ratios are low: from 7×10^{-4} on sample 13 to 0.024 in 12. It is related to the fact that deposits on the liner and limiters are at poor thermal contact with the underlying substrate and, therefore, the fuel content is strongly affected by plasma operation. Hydrogen constitutes the majority of the released gas. This result is consistent with earlier studies of deposits [7,33,38] and it is related to at least three factors: (i) presence of protium in the tokamak either as a fuelling or residual gas and consequently hydrogen co-deposition on the walls, (ii) isotope exchange between deuterium and hydrogen from water vapour while co-deposits are exposed to air and (iii) adsorption of water vapour on porous structure of deposits.

Concluding remarks

A comprehensive survey of dust after the final shut-down of TEXTOR has been performed. An important point is that there was fairly little loose matter (a few grams only) that could be collected from PFC and the liner bottom by sweeping, therefore samples were obtained by scraping co-deposits loosely bound to substrates in various parts of the machine. From the microstructure point of view several distinct categories of dust have been identified. As expected, carbon-based deposits of stratified, granular and mixed type of structure were dominating, but the major interest in the study was on metal constituents. Nickel-rich alloys (from the Inconel TEXTOR liner) and iron-based ones were the main components of metal-containing dust. Molybdenum and tungsten debris were also found. Metal species were in the form of small particles, small spheres, flakes and splashes which formed "comet"-like structures clearly indicating directional effects in the impact on surfaces of plasma-facing components.

Acknowledgement

This work has been carried out within the framework of the EUROfusion Consortium and has received funding from the European Union's Horizon 2020 research and innovation programme under grant agreement number 633053. The views and opinions expressed herein do not necessarily reflect those of the European Commission. The work has been partly funded by the Swedish Research Council (VR) through contract no. 621-2009-4138.

References

[1] Winter J, 1998 *Plasma Phys. Control. Fusion* **40** 1201

[2] Winter J and Gebauer G 1999 *J. Nucl. Mater.* **266-269** 228

[3] Rubel M *et al* 2001 *Nucl. Fusion* **41** 1087

[4] Linke J *et al* 2001 *Phys. Scr.* **T9**1 36

[6] Fortuna E *et al* 2007 *J. Nucl. Mater*. **367-370** 1507

[7] Ivanova D *et al* 2009 *Phys. Scr*. **T138** 014012

[8] Ivanova D *et al* 2011 *J. Nucl.* Mater **415** S801

[9] Rohde V *et al* 2009 *Phys. Scr.* **T138** 014024

[10] Fortuna *et al* 2014 *Phys. Scr.* **T159** 014066

[11] Balden M *et al* 2014 *Nucl. Fusion* **54** 073010

[12] Pegourie B *et al* 2013 *J. Nucl. Mater.* **438** S120

[13] Braams B 2012 Characterisation of Size, Composition and Origins of Dust in Fusion Devices, *http://www-nds.iaea.org/reports-new/indc-reports*

[14] Counsell G *et al* 2006 *Plasma Phys. Control. Fusion* **48** B189

[15] Roth J *et al* 2009 *J. Nucl. Mater.* **390-391** 1

[16] Philipps V *et al* 1998 *J. Nucl. Mater.* **258-263** 858

[17] Tanabe T *et al* 1994 *J. Nucl. Mater.* **212-215** 1370

[18] Rubel M *et al* 1996 *J. Nucl. Mater.* **249** 116

[19] Tanabe T *et al* 2000 *J. Nucl. Mater.* **283-287** 355

[20] Rubel M *et al* 2000 *J. Nucl. Mater.* **283-287** 1089

[21] Hirai T *et al* 2003 *Phys. Scr.* **T103** 59

[22] Hirai T *et al* 2003 J *J. Nucl. Mater.* **313-316** 67

[23] Sergienko G *et al* 2007 *Phys. Scr.* **T128** 81

[24] Sergienko G *et al* 2007 *J. Nucl. Mater.* **363-365** 96

[25] Rubel M *et al* 2008 *Fusion Des. Eng.* **83** 1049

[26] Psoda M *et al* 2009 *J. Nucl. Mater.* **386-388** 740

[27] Pospieszczyk A *et al* 2001 *J. Nucl. Mater.* **290-293** 947

[28] Fortuna E *et al* 2007 *Phys. Scr.* **T128** 162-165

[29] Litnovsky A *et al* 2013 *J. Nucl. Mater.* **438** S126

[30] Rubel M *et al* 2013 *J. Nucl. Mater.* **438** S170

[31] Rubel M *et al* 2015 *J. Nucl. Mater.* http://dx.doi.org/10.1016/j.jnucmat.2014.11.074

[32] Weckmann A *et al* These Proceedings

[33] Rubel M *et al* 2003 *Phys. Scr.* **T103** 20

[34] Winter J *et al* 1989 *J. Nucl. Mater.* **162-164** 713

[35] Wienhold P *et al* 2003 *J. Nucl. Mater.* **313-316** 311

[36] Kirschner A *et al* 2005 *Fusion Sci. Technol* . **47** 146

[37] Litnovsky A *et al* 2011 *J. Nucl. Mater.* **415** S289

[38] Rubel M *et al* 2001 *J. Nucl. Mater.* **290-293** 473